Rho-family GTPases require the Arp2/3 complex to stimulate actin polymerization in *Acanthamoeba* extracts

R. Dyche Mullins* and Thomas D. Pollard

Background: Actin filaments polymerize *in vivo* primarily from their fast-growing barbed ends. In cells and extracts, GTPγS and Rho-family GTPases, including Cdc42, stimulate barbed-end actin polymerization; however, the mechanism responsible for the initiation of polymerization is unknown. There are three formal possibilities for how free barbed ends may be generated in response to cellular signals: uncapping of existing filaments; severing of existing filaments; or *de novo* nucleation. The Arp2/3 complex localizes to regions of dynamic actin polymerization, including the leading edges of motile cells and motile actin patches in yeast, and *in vitro* it nucleates the formation of actin filaments with free barbed ends. Here, we investigated actin polymerization in soluble extracts of *Acanthamoeba*.

Results: Addition of actin filaments with free barbed ends to *Acanthamoeba* extracts is sufficient to induce polymerization of endogenous actin. Addition of activated Cdc42 or activation of Rho-family GTPases in these extracts by the non-hydrolyzable GTP analog GTPγS stimulated barbed-end polymerization, whereas immunodepletion of Arp2 or sequestration of Arp2 using solution-binding antibodies blocked Rho-family GTPase-induced actin polymerization.

Conclusions: For this system, we conclude that the accessibility of free barbed ends regulates actin polymerization, that Rho-family GTPases stimulate polymerization catalytically by *de novo* nucleation of free barbed ends and that the primary nucleation factor in this pathway is the Arp2/3 complex.

Address: The Salk Institute for Biological Studies, 10010 N. Torrey Pines Road. La Jolla, California, 92037, USA.

Present address: *Department of Cellular and Molecular Pharmacology, University of California, San Francisco, 513 Parnassus Avenue, San Francisco, California 94143, USA.

Correspondence: R. Dyche Mullins
E-mail: dyche@sbl.salk.edu

Received: 15 December 1998
Revised: 22 February 1999
Accepted: 9 March 1999

Published: 8 April 1999

Current Biology 1999, 9:405–415
http://biomednet.com/elecref/0960982200900405

 ISSN 0960-9822

Background

Polymerization of actin filaments at their fast-growing barbed ends drives the extension of the leading edge in motile cells [1–4]. To establish cell polarity and to generate directed cell motility in response to external cues like chemoattractants and repellants [5] or to the extracellular matrix [6], actin polymerization must somehow be controlled by cellular signaling pathways. To generate sustained motility, actin subunits must continuously cycle [7] from a diffusible monomeric pool in the cytoplasm [8] onto the barbed ends of filaments at the leading edge and, by filament depolymerization, back to the monomeric pool [9]. Formally, the initiation of actin polymerization could be regulated in one of two ways, either by regulating the accessibility of barbed ends or by regulating the competence of actin monomers to polymerize. A commonly accepted hypothesis is that exposure of free barbed ends is sufficient to induce actin polymerization [10], but this has never been demonstrated directly and has been challenged by recent results [11].

Exposed barbed ends are generated *in vivo* by three mechanisms: uncapping existing actin filaments; severing of existing filaments; and *de novo* nucleation. Membrane polyphosphoinositides dissociate the barbed-end capping factors capping protein [12] and gelsolin [13] from barbed ends, but this mechanism does not appear to be involved in chemotaxis of motile cells [14]. Actin depolymerizing factors of the ADF/cofilin family sever ADP–actin filaments without capping them [15], but this appears to contribute more to filament disassembly than to polymerization [16]. In platelets, calcium stimulates gelsolin to sever and cap filaments and this process, coupled with uncapping, creates new barbed ends [17]. The capping factors gelsolin and capping protein stimulate the formation of new pointed ends, but, until recently, no cellular factors were known to make new barbed ends.

Most environmental cues that stimulate actin polymerization appear to act through the Rho family of small GTP-binding proteins [18]. In intact cells, cytoskeletal organization [19] and chemotaxis [20] are regulated by Rho-family GTPases. In cell extracts, addition of activated Cdc42 (a Rho-family GTPase) or activation of endogenous GTPases by the non-hydrolyzable GTP analog GTPγS induces a burst of actin polymerization and this effect requires phospholipids that enhance guanine nucleotide exchange or that aggregate small GTPases [21–23]. The mechanism by which Rho-family GTPases, in particular Cdc42, stimulate barbed-end actin polymerization, however, is unknown.

The Arp2/3 complex, which contains the actin-related proteins Arp2 and Arp3 and five other subunits, is the only cellular component known to nucleate filaments with free barbed ends [24,25]. This complex is essential in yeast [26,27] and is required for actin assembly on the surface of intracellular pathogens such as *Listeria* [28]. Nucleation of new filaments by *Listeria* is interesting in its own right, but is constitutive and independent of small GTPases, so it is not necessarily informative regarding the response of cells to external stimuli.

Here, we have investigated actin polymerization in soluble extracts of *Acanthamoeba castellanii*. These extracts maintain a large, stable pool of unpolymerized actin and respond to addition of filaments, GTPγS or activated Cdc42 with a transient burst of actin polymerization. The time course of the response to added filaments indicates that polymerization is limited by pseudo-first-order capping of barbed ends. Addition of the Rho guanine nucleotide dissociation inhibitor RhoGDI, which inhibits activation of Rho-family GTPases, or inhibition of the Arp2/3 complex, the only known barbed-end nucleating factor in *Acanthamoeba*, blocks the response of actin to GTPγS. These data indicate that Rho-family GTPases stimulate actin polymerization through nucleation by the Arp2/3 complex.

Results

Composition of *Acanthamoeba* extracts

Concentrated, soluble extracts of *Acanthamoeba* contained 70 μM total actin, as detected by immunoblotting, approximately 70 μM profilin (D.A. Kaiser and T.D.P., unpublished observations) and 0.6 μM Arp2/3 complex. The actin concentration was about a third of the concentration that has been measured in intact cells [29]. When the extract was fractionated by gel filtration and assayed by immunoblotting, all the Arp2 and Arp3 was present exclusively as part of a large particle, which has a Stokes' radius of 5.4 nm, identical to that of the purified complex (J.F. Kelleher and R.D.M., unpublished observations).

Characterization of the actin pool in extracts

Gel-filtration chromatography revealed that all of the 70 μM actin in the cold, high-speed supernatant was monomeric and was mostly bound to profilin (D.A. Kaiser and T.D.P., unpublished observations), but as observed previously [30,31], about 30% of the actin polymerized when the extract was warmed to room temperature. Rhodamine–phalloidin binding and SDS–PAGE analysis of high-speed supernatants gave the same measurement of the amount of filamentous actin. After dilution of these extracts 1:10 into P buffer (see Materials and methods), the pools of 5 μM actin monomer and 2 μM actin filaments were stable for at least 3000 seconds (Figures 1a,2a and data not shown), even though the monomer concentration was well above the 0.1 μM critical concentration. We therefore conclude that regulatory proteins suppress spontaneous nucleation and/or elongation. By using at least 10-fold diluted extracts we lowered the concentration of actophorin, the most abundant protein known to quench pyrene fluorescence, to approximately 0.7 μM, far lower than the total concentration of actin, approximately 7 μM.

Figure 1

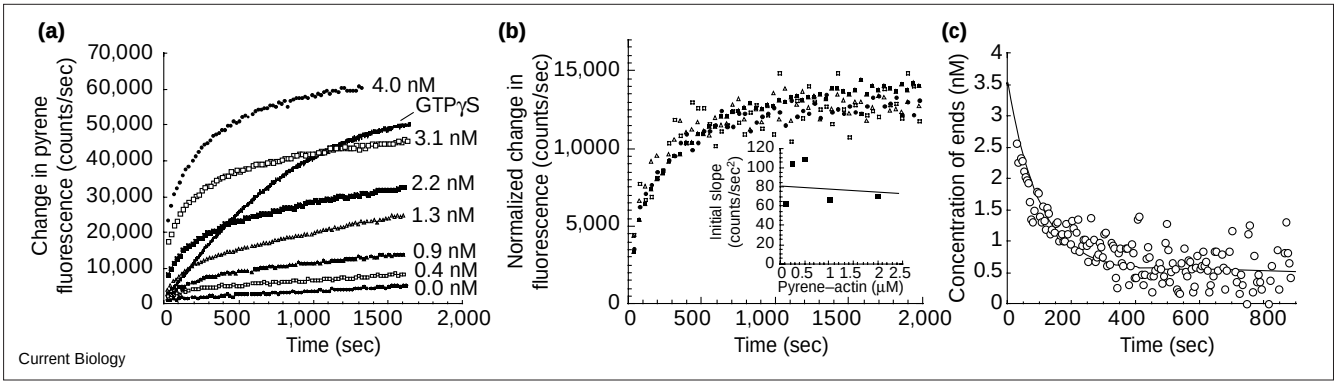

Elongation of exogenous actin filaments in *Acanthamoeba* extracts. (a) Time course of the change in the pyrene fluorescence of extracts with 500 nM pyrene–actin and either 270 μM GTPγS or a range (0–4 nM) of concentrations of polymerized unlabeled amoeba actin filaments. The concentration of ends was calculated by performing parallel elongation experiments with varying concentrations of purified actin. The experiment was carried out at 24°C and the extract was diluted 1:15 with varying amounts of pyrene–actin into 100 mM KCl, 340 mM sucrose, 2 mM $MgSO_4$, 1 mM $MgCl_2$, 2 mM EGTA, 1 mM ATP, 1 mM dithiothreitol (DTT), 20 mM imidazole. (b) Time course of the change in fluorescence of extracts with 1 nM exogenous filament ends and varying concentrations of pyrene–actin (0.1 μM open squares, 0.2 μM open triangles, 0.5 μM filled circles, 1.0 μM filled triangles). The inset shows the initial rate of change in pyrene fluorescence as a function of pyrene–actin concentration. (c) Time course of the decline in free barbed ends in a cell extract calculated from the 4 nM barbed end data set in (a) according to equation 6 (see Materials and methods).

Figure 2

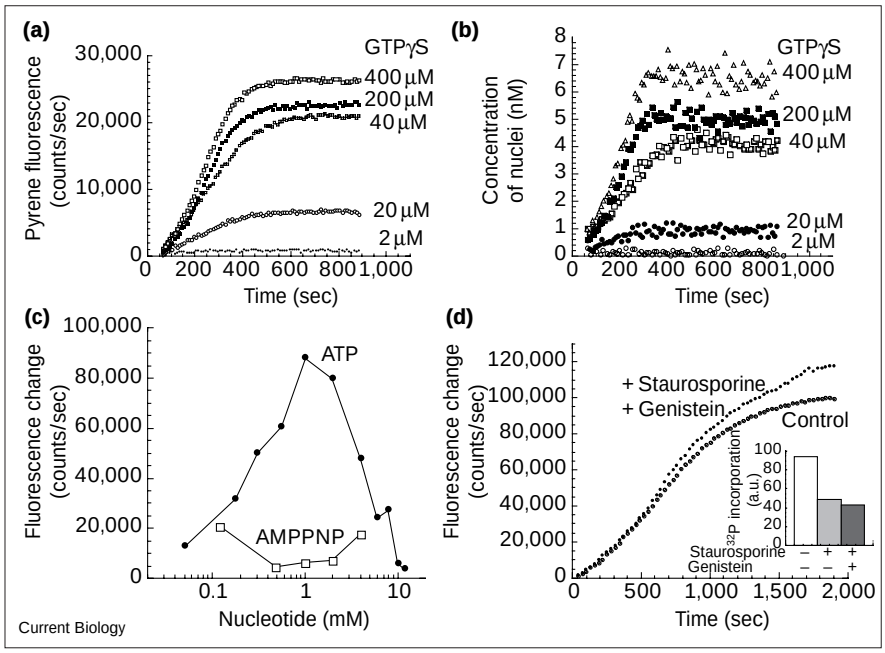

GTPγS-stimulated polymerization monitored by change in fluorescence of added pyrene–actin. The experiment was carried out at 24°C; amoeba extracts were diluted 1:10 in 100 mM KCl, 340 mM sucrose, 2 mM $MgSO_4$, 1 mM $MgCl_2$, 2 mM EGTA, 1 mM DTT, 20 mM imidazole, pH 7.0. The concentrations of ATP and GTPγS were varied as indicated. Pyrene-labeled amoeba actin was added to 100 nM. (a) Polymerization of pyrene–actin in amoeba extracts (1 mM ATP) stimulated by GTPγS at concentrations ranging from 2 μM to 400 μM as indicated. (b) Cumulative concentration of filament nuclei produced by GTPγS stimulation calculated from the data in (a) according to equation 9. (c) Dependence of maximum change in pyrene fluorescence induced by 200 μM GTPγS on the concentration of ATP or the non-hydrolyzable ATP analog AMPPNP as indicated. (d) Actin polymerization in the presence and absence of kinase inhibitors. The experiment was performed in the same way as (a) except that extracts were diluted 1:20. Extracts were stimulated with 200 μM GTPγS. The inset shows the effects of 3 μM staurosporine or 3 μM staurosporine and 5 μM genistein on ^{32}P-labeling of proteins in GTPγS-stimulated amoeba extracts.

Addition of actin filaments to the extract induced polymerization of endogenous actin (Figure 1a). We followed polymerization by the change in fluorescence intensity of a trace amount of pyrene-labeled *Acanthamoeba* actin. The concentration of pyrene-labeled actin (100–500 nM) was only 1–10% of the endogenous actin concentration. Skeletal-muscle actin behaves very differently from cytoplasmic actin in *Acanthamoeba* extracts [32], so we used fluorescently labeled amoeba cytoplasmic actin in all assays. Profilin (and possibly other actin-binding proteins) has a 10-fold lower affinity for pyrene–actin than for unlabeled actin [33], so to rule out the possibility that pyrene–actin polymerized preferentially in these extracts, we measured polymerization at many different concentrations of added pyrene–actin. Neither the time course (Figure 1b, inset) nor the amplitude of the fluorescence change (corrected for dilution, Figure 1b) varied with pyrene–actin concentration, indicating that the pyrene fluorescence reflected the kinetics of polymerization of endogenous actin. The rate and extent of polymerization depended on the concentration of added filaments. At high filament concentrations, essentially all of the monomer pool polymerized, showing that all of this pool was competent for polymerization. At lower filament concentrations, polymerization slowed before the subunit pool was exhausted (Figure 1a).

The slowing of polymerization in the presence of a pool of competent actin monomers (Figure 1a) indicated that filament elongation was terminated prematurely, most likely by capping. Kinetic analysis of the time course of polymerization over a range of added filament concentrations enabled us to define this termination mechanism quantitatively. We measured the rate of capping by first calculating the number of free barbed ends at each point during the experiment:

$$[E] = \frac{d[F]}{dt}\frac{1}{k_+[A] - k_-} \quad (1)$$

where [E], [F] and [A] are instantaneous concentrations of barbed ends, filamentous actin and polymerizable monomers, respectively (Figure 1c) and k_+ and k_- are the monomer association and dissociation rate constants. We considered all monomeric actin in the extract to be capable of polymerization.

The concentration of free barbed ends in the extract declined exponentially after addition of filaments to a limiting value of about 15% of the starting value (Figure 1c). We consider this limiting value to approximate the steady-state concentration of free barbed ends. We used the observed rate constant of capping (k_{obs}) and the concentrations of free ends at time zero (E_0) and at the steady state (E_{ss}) to calculate the forward and reverse rate constants of capping factors in the extract by:

$$k_{c-} = \left(\frac{E_{ss}}{E_0}\right)k_{obs} \quad (2)$$

$$k_{c+}[C] = \left(1 - \frac{E_{ss}}{E_0}\right) k_{obs} \quad (3)$$

where k_{c-} and k_{c+} are the average forward and reverse rate constants and [C] is the apparent concentration of capping factors. From this, we calculate that $k_{c-} = 1.2 \times 10^{-3} \pm 0.2 \times 10^{-3}$ sec^{-1} and $k_{c+}[C] = 7.3 \times 10^{-3} \pm 0.9 \times 10^{-3}$ sec^{-1}.

Capping protein is the major barbed-end capping factor detectable in neutrophil extracts [34] and the only one known in *Acanthamoeba* [35]. Our value for k_{c-} agrees well with the dissociation rate constant of 1.9×10^{-3} sec^{-1} that was obtained from similar measurements of capping-protein kinetics in neutrophil extracts [34] and 0.4×10^{-3} sec^{-1} that was measured for purified capping protein [12]. From estimates of capping-protein concentration in our extracts [36], we calculated a forward rate constant of 0.4 μM^{-1} sec^{-1}. This value is 10-fold lower than the forward rate constant of 3.5 μM^{-1} sec^{-1} measured by Schafer *et al.* [12] for the binding of vertebrate capping protein to vertebrate skeletal muscle. The rate constant for the binding of amoeba capping protein to amoeba actin may be lower or factors in the extract, possibly phospholipids, may have reduced the concentration of active capping protein.

Effect of GTPγS on actin in the extract

Addition of GTPγS to dilute extracts induced actin polymerization, which we followed quantitatively by monitoring the change in fluorescence intensity of a trace of pyrene-labeled *Acanthamoeba* actin (Figure 2a). Pelleting the filaments and assaying the pellets by SDS–PAGE and Coomassie-blue staining or by rhodamine–phalloidin fluorescence confirmed the results of the pyrene fluorescence assay (data not shown).

After an initial lag, which was not seen with added actin filaments, GTPγS induced an increase in pyrene fluorescence, which reached a plateau value within 500 seconds (Figure 2a). Cytochalasin D — which, at low concentrations, caps the barbed ends of actin filaments — inhibited GTPγS-stimulated actin polymerization in a concentration-dependent manner. Maximal inhibition was 92% at 40 nM cytochalasin D, so we conclude that GTPγS-stimulated polymerization occurs predominantly at exposed barbed ends. The rate and extent of the change in fluorescence depended on the concentration of GTPγS. At 200 μM GTPγS, 86% of the total actin polymerized. The final extent of polymerization at high concentrations of filaments or GTPγS was similar, showing that GTPγS was not simply releasing sequestered actin monomers. If we first pelleted the filamentous actin in the extract, GTPγS still induced polymerization, indicating that severing or uncapping was not required for GTPγS-induced polymerization. GTPγS did not alter the phospholipid composition as detected by thin-layer chromatography (our unpublished observations).

The time course of polymerization (Figure 2a) and the time course of capping (Figure 1c) were sufficient to calculate the concentration of filament nuclei produced by stimulation with GTPγS. We estimated that, in extracts diluted 1:10 (corresponding to an approximate 1:15 dilution from cytoplasmic concentrations), addition of 200–400 μM GTPγS induced formation of approximately 5–7 nM barbed ends (Figure 2b). This is consistent with the data in Figure 1a, in which 270 μM GTPγS produced a total amount of actin polymerization similar to that obtained following addition of 4 nM free barbed ends. The rate of formation of filament nuclei increased with increasing concentrations of GTPγS. The time at which nucleation terminated, however, was relatively constant and did not vary with the concentration of GTPγS.

ATP requirement

GTPγS-stimulated actin polymerization in dilute extracts required hydrolyzable ATP. The plateau fluorescence of pyrene–actin increased with ATP concentration to a maximum at 1 mM ATP (Figure 2c). ATP concentrations of more than 1 mM inhibited for actin polymerization. The non-hydrolyzable ATP analog AMPPNP did not substitute for ATP, suggesting that ATP hydrolysis was required for the response to GTPγS.

To determine whether protein phosphorylation was involved, we tested the effects of the broad-spectrum kinase inhibitors staurosporine and genistein on polymerization. We monitored the effectiveness of these inhibitors by adding [γ-^{32}P]ATP to cell extracts that had been diluted 1:15 and detecting phosphorylated proteins in the presence and absence of inhibitors by SDS–PAGE and autoradiography. At the highest kinase inhibitor concentrations tested — 3 μM staurosporine plus 5 μM genistein — the inhibitors decreased total protein phosphorylation in both the presence and the absence of GTPγS by more than 50% but had no effect on the kinetics or extent of GTPγS-stimulated actin polymerization (Figure 2d).

Participation of small GTP-binding proteins in actin assembly

Two lines of evidence show that small GTPases of the Rho family mediate the effect of GTPγS on actin polymerization in amoeba extracts. First, recombinant RhoGDI, an inhibitor of the exchange of GDP for GTP on Rho-family GTPases [37], inhibited GTPγS-stimulated polymerization (Figure 3a). Half-maximal inhibition occurred with 60 nM RhoGDI and inhibition was complete above 300 nM. Second, addition of GTPγS-loaded Cdc42, a member of the Rho family that is known to induce actin polymerization in intact cells [38] and cell extracts [21], induced actin polymerization in amoeba extracts (Figure 3b). The rate of Cdc42-induced polymerization was maximal at 100 nM Cdc42 but decreased at concentrations above 200 nM (data not shown). This induction of polymerization could not be

Figure 3

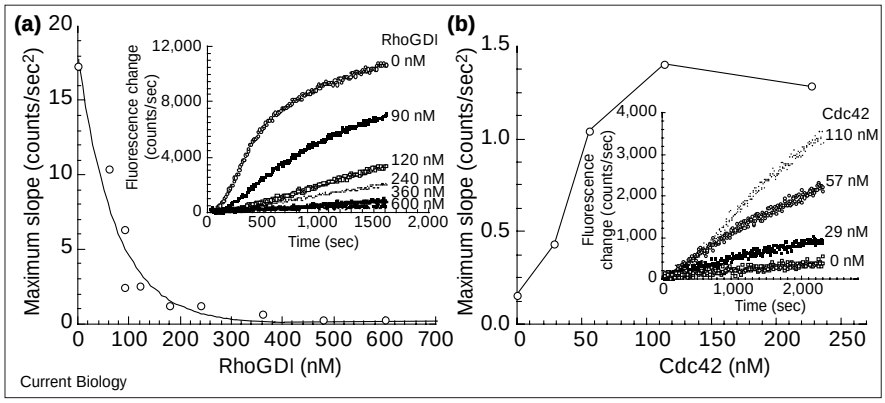

Rho-family GTPases mediate actin polymerization in *Acanthamoeba* extracts. (a) The effect of RhoGDI on GTPγS-induced actin polymerization in extracts. The experiment was carried out at 24°C; amoeba extracts were diluted 1:20 into 200 μM GTPγS, 100 mM KCl, 340 mM sucrose, 2 mM $MgSO_4$, 1 mM $MgCl_2$, 2 mM EGTA, 1 mM DTT, 20 mM imidazole, pH 7.0 containing varying concentrations of RhoGDI as indicated and 680 nM pyrene-labeled amoeba actin. The maximum rate of change of pyrene fluorescence induced by GTPγS is plotted as a function of RhoGDI concentration. The inset shows the time course of the change in pyrene fluorescence at the various concentrations of RhoGDI. (b) Stimulation of actin polymerization in extracts by Cdc42. The experimental conditions were the same as those in (a) but with no RhoGDI and varying concentrations of Cdc42 as indicated. The maximum rate of change of pyrene fluorescence in the first 2,000 sec of the assay is plotted as a function of Cdc42 concentration. The inset shows the time course of the change in pyrene fluorescence at the various concentrations of Cdc42.

due to the GTPγS that had been added with the Cdc42, because, although Cdc42 was activated in buffer containing a three-fold excess of GTPγS, the concentration of GTPγS added with the Cdc42 at maximally effective concentrations of Cdc42 was less than 300 nM, which, by itself, had no detectable effect on actin polymerization.

Requirement for the Arp2/3 complex in G-protein-mediated actin polymerization

We used solution-binding antibodies and immunodepletion to determine the role of the Arp2/3 complex in G-protein-mediated actin polymerization in amoeba extracts. Anti-Arp2 antibodies had a profound, concentration-dependent effect on actin polymerization stimulated by GTPγS (Figure 4b,c) or Cdc42 (Figure 4d). The effect of the antibodies saturated at 200 μg/ml and inhibited GTPγS-stimulated polymerization by 80% (Figure 5c). Anti-Arp3 antibodies served as a control because they did not bind native Arp2/3 complex in solution (Figure 6). These antibodies had no effect on actin polymerization stimulated by GTPγS or Cdc42 at any concentration tested (Figure 4a,c).

Figure 4

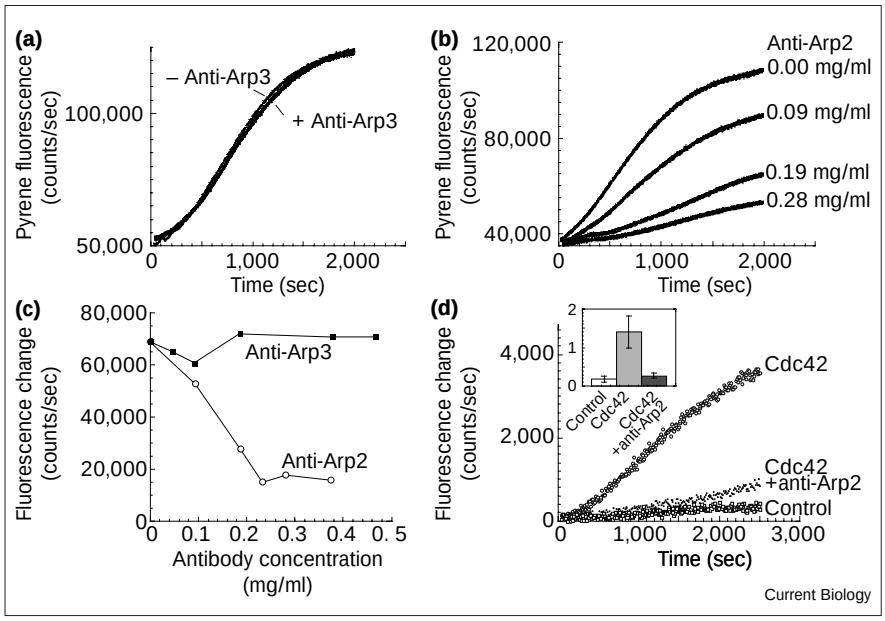

Effect of anti-Arp2 and anti-Arp3 antibodies on the GTPγS-induced actin polymerization in diluted extracts. The experimental conditions were the same as those in Figure 3. (a) Time course of the change in fluorescence of diluted extracts (1:15) with 500 nM pyrene–actin stimulated with 270 μM GTPγS in the absence or presence of 0.38 mg/ml anti-Arp3 antibody. (b) A similar time course of change in fluorescence as in (a) but with varying concentrations of anti-Arp2 antibody as indicated. (c) Dependence of the extent of GTPγS-stimulated polymerization at 2,000 sec after stimulation on the concentrations of anti-Arp2 and anti-Arp3 antibodies. (d) Inhibition of Cdc42-stimulated actin polymerization by anti-Arp2 antibodies. The inset shows the maximum rate of change of pyrene fluorescence in extract alone (control), with 100 nM Cdc42, or with 100 nM Cdc42 and 980 μg/ml anti-Arp2 antibodies. Results are averages of three measurements and error bars represent standard deviation.

Figure 5

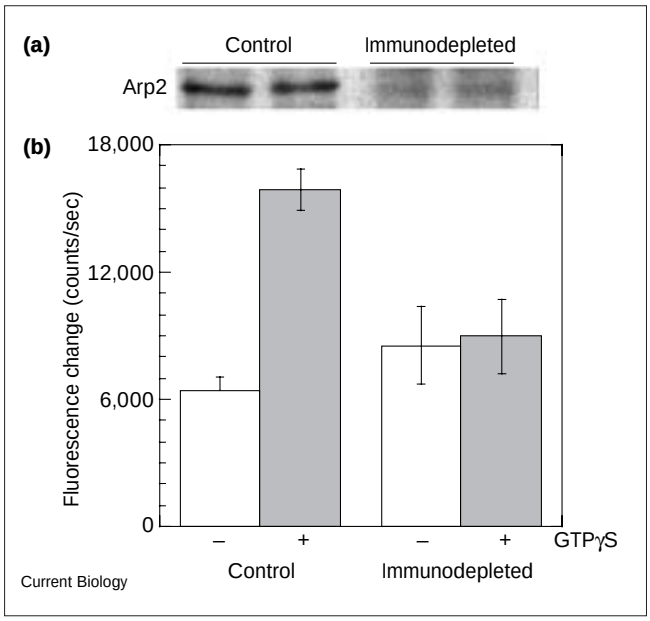

Effect of immunodepletion of Arp2/3 complex on GTPγS-stimulated actin polymerization in *Acanthamoeba* extracts. (a) Duplicate immunoblots of control and immunodepleted cell extracts probed with anti-Arp2 antibodies. The diluted extract was incubated with 4 mg/ml anti-Arp2 antibodies for 1 h at 4°C and antibody–antigen complexes were removed by binding to protein-A–Sepharose beads and filtration through glass wool. (b) GTPγS-stimulated actin polymerization in mock-immunodepleted and immunodepleted extracts measured by change in pyrene fluorescence 600 sec after addition of 270 μM GTPγS. The experimental conditions were the same as those in Figure 2a. Mock-immunodepleted extracts (control) responded to addition of GTPγS with an increase in the rate of actin polymerization whereas immunodepleted extracts no longer responded to stimulation.

Immunodepletion of the Arp2/3 complex confirmed its importance for the response to GTPγS and Cdc42 (Figure 5). Anti-Arp2 antibodies removed more than 90% of the Arp2/3 complex (Figure 5a) and decreased GTPγS-stimulated polymerization to levels as low as those in the absence of GTPγS stimulation (Figure 5b). Total protein concentration in the extract, estimated by Ponceau-red staining of immunoblots, was unchanged. Mock immunodepletion increased the rate of polymerization in unstimulated extracts, presumably because some capping activity was lost. Addition of purified Arp2/3 complex to immunodepleted extracts, however, did not restore responsiveness to GTPγS (data not shown). Activated Cdc42 had no effect on the ability of purified Arp2/3 complex to nucleate actin-filament formation (data not shown), suggesting that the connection between Cdc42 and the Arp2/3 complex in extracts is not direct but is mediated by another factor(s).

Discussion

We have shown that *Acanthamoeba* extracts retain a stable pool of monomeric actin that can be induced to polymerize by activation of Rho-family GTPases. This behavior is similar to that observed in extracts from *Dictyostelium* [11,21], neutrophils [21,22] and *Xenopus* oocytes [23], and makes *Acanthamoeba* a good system for studying the endogenous signaling pathways that regulate actin polymerization. From kinetic analysis of GTPγS-stimulated polymerization, we conclude that activated Rho-family GTPases act via the Arp2/3 complex to produce a constant rate of formation of new barbed ends. Polymerization is limited by two factors: barbed-end capping and termination of nucleation. Capping of free barbed ends can be described by a single exponential equation as predicted for a simple bimolecular reaction. In response to stimulation, barbed ends are produced at a constant rate for 300–400 seconds (in 10-fold diluted extracts) and then nucleation abruptly terminates (Figure 2b), probably because of a negative feedback or intrinsic timing mechanism. Purified Cdc42 requires the Arp2/3 complex to stimulate polymerization in extracts but does not directly activate purified Arp2/3 complex, suggesting that other factors downstream of Cdc42 interact with this complex.

Actin dynamics in cell extracts

Despite early skepticism [39], we now know that significant portions of the regulatory pathways that control actin polymerization in intact cells can be preserved and studied in cell extracts. An underappreciated aspect of experiments performed using extracts is that foreign actin may not behave in the same way as the endogenous cytoplasmic actin. For example, skeletal-muscle actin filaments depolymerize rapidly in *Acanthamoeba* extracts, whereas added amoeba filaments are stable [32]. To our knowledge, this is the first study of G-protein-mediated actin polymerization in live cells or cell extracts to rely exclusively on non-muscle, cytoplasmic actin for all assays.

A widely held view is that, *in vivo*, actin polymerization is regulated by the accessibility of barbed ends rather than the availability of polymerization-competent monomers. We tested this mechanism directly in cell-free extracts by adding various concentrations of barbed ends and measuring the incorporation of endogenous actin. Endogenous actin could elongate exposed barbed ends until they were capped. As expected from a simple bimolecular reaction of an excess of capping protein with barbed ends, the decline in the number of barbed ends with time follows a single exponential curve (Figure 1c). The final extent of polymerization therefore depended on the concentration of barbed ends added to the extract (Figure 1a).

The large pool of actin subunits required to drive motility appears to be kinetically trapped in an unpolymerized state by a combination of filament capping and suppression of spontaneous nucleation. *Acanthamoeba* (along with other protozoa and yeast) probably represent the simplest case, in which most or all of the unpolymerized actin is bound to

Figure 6

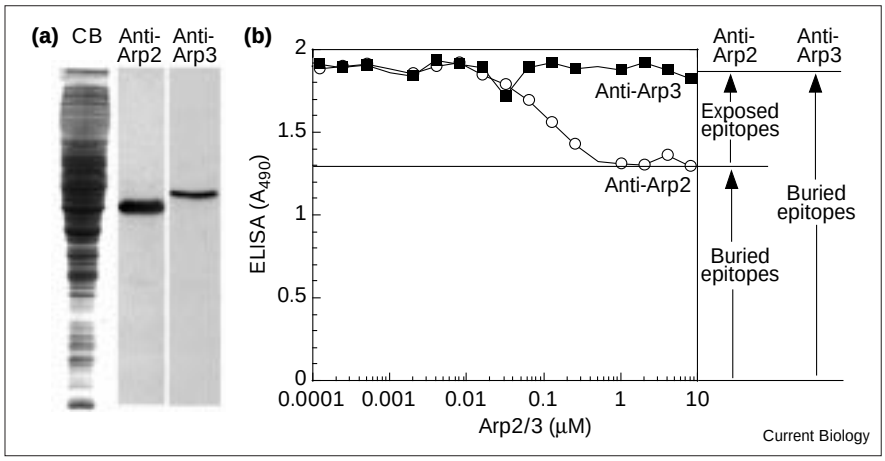

Characterization of anti-Arp2 and anti-Arp3 antibodies. (a) Immunoblots of soluble *Acanthamoeba* extracts probed with anti-Arp2 and anti-Arp3 antibodies. Concentrated extract (2 μl) was subjected to 13.75% SDS–PAGE and the gel was either stained with Coomassie blue (CB) or electroblotted to nitrocellulose and probed with anti-Arp2 or anti-Arp3 antibodies. (b) Competitive binding of the soluble Arp2/3 complex to anti-Arp2 and anti-Arp3 antibodies. One third of the anti-Arp2 antibodies recognize native epitopes exposed on the surface of the Arp2/3 complex but none of the anti-Arp3 antibodies recognizes surface-exposed epitopes. The Arp2/3 complex was adsorbed to microtiter-plate wells and detected by enzyme-linked immunosorbent assay (ELISA) using anti-Arp2 or anti-Arp3 antibodies at the same titer. Varying concentrations of native Arp2/3 complex were pre-incubated for 1 h at 24°C with the antibody to compete for binding with the denatured Arp2/3 complex adsorbed to the plastic wells.

profilin, a small protein that binds tightly to Mg–ATP–actin monomers [41]. Profilin suppresses spontaneous filament formation and prevents growth at the slow-growing pointed ends of actin filaments [42], but profilin–actin complexes elongate barbed ends nearly as quickly as free actin [42,43]. The concentration of profilin in *Acanthamoeba* (100 mM) [44] is high enough to bind to most unpolymerized actin in the cell. In addition to profilin, vertebrate cells contain thymosin-β4, which sequesters monomers. Actin bound to thymosin-β4 is not competent for polymerization [45,46] but profilin can shuttle actin monomers from thymosin-β4 onto exposed barbed ends [47].

GTPγS-stimulated actin polymerization

We have shown that small GTPases regulate actin polymerization in extracts of *Acanthamoeba*. The complete inhibition by RhoGDI that we observed indicates that all of the GTPγS-initiated signaling flows through the Rho-family GTPases. At early time points, GTPγS produced filament nuclei at a remarkably constant rate. Nucleation stopped abruptly at about 325 seconds after stimulation (Figure 2b). The rate of nucleation increased as the concentration of GTPγS increased, but the time at which nucleation stopped was constant, being independent of added GTPγS or the concentration of actin polymerized. The system appears to be adapted to produce a graded response to signals by varying the nucleation rate rather than by instantaneously producing a number of filament ends proportional to the stimulus. This difference was particularly apparent when we directly compared GTPγS-stimulated polymerization with that stimulated by the addition of a fixed number of filament nuclei (Figure 1a). Both 3.1 nM added filament ends and 270 μM GTPγS induce approximately the same amount of actin polymerization. When pre-formed filaments were added, the initial rate of polymerization was maximal and decreased immediately and monotonically because of capping. When GTPγS was added, however, the initial polymerization rate was low but increased or remained constant for the first 300–400 seconds as free barbed ends were formed. We do not know the molecular mechanism behind this linear nucleation rate, but it probably reflects catalytic formation of nuclei downstream of the activated GTPase. This activity appears to be blocked by an intrinsic timing or negative feedback mechanism.

The polymerization of actin in extracts is controlled by a balance between nucleation and capping. For a constant rate of nucleation in the presence of capping proteins, the rate of change of free barbed ends ($[E]_{free}$) is described by the differential equation:

$$\frac{d}{dt}[E]_{free} = R_N - k_{c+}[C][E]_{free} \quad (4)$$

where R_N is the nucleation rate, k_{c+} the rate constant for capping and [C] the concentration of capper. At a constant nucleation rate, the number of free barbed ends increases until the rate at which they are capped ($k_{c+}[C][E]_{free}$) equals the rate at which they are formed (R_N). Under pseudo-first-order conditions, in which [C] is in excess of filament end concentration [E], we can solve this equation to give the concentration of free barbed ends as a function of time:

$$[E]_{free} = \frac{R_N}{k_{c+}[C]}(1 - e^{-k_{c+}[C]t}) \quad (5)$$

This equation is a single exponential, in which the amplitude is directly proportional to the nucleation rate

and the time-course depends solely on the pseudo-first-order rate constant, $k_{c+}[C]$. It applies only to conditions where capping protein concentration is in excess of barbed end concentration.

Although we have found that added actin filaments readily elongate in *Acanthamoeba* extracts, a recent report [11] suggests that in neutrophil extracts exogenous actin (muscle actin filaments and spectrin–actin seeds) elongate much more slowly than endogenous filaments generated by Cdc42. Other explanations of the data in that study [11] are that exogenous seeds depolymerize or are capped more quickly than endogenous filaments. The time course of the appearance of free barbed ends in the other study [11] is well fitted by our equation 5 when the capping rate determined for *Acanthamoeba* extracts is used (data not shown). This implies that the time for half of the Cdc42-nucleated filaments to be capped (the half-time) in neutrophil extracts is of the order of 120 seconds. The half-time that was measured for capping of spectrin–actin seeds in neutrophil extracts [11] was much shorter, less than 6 seconds, suggesting that spectrin–actin seeds are capped more quickly than endogenous actin filaments. This difference may be mediated by Cdc42, but the possibility that spectrin–actin seeds are somehow different from endogenous actin filaments has not been ruled out.

The role of the Arp2/3 complex in GTPγS-stimulated actin polymerization

Ma *et al.* [48] recently reported that, in *Xenopus* extracts, the Arp2/3 complex and an unidentified factor(s) are sufficient to support Cdc42-mediated actin polymerization. Here, we have shown that the Arp2/3 complex is also necessary for all Rho-family G-protein-mediated actin polymerization in amoeba extracts. Two experiments showed that the Arp2/3 complex was responsible for GTPγS-stimulated actin polymerization in our extracts: firstly, monospecific antibodies against Arp2 that bind the Arp2/3 complex in solution inhibited both Cdc42- and GTPγS-stimulated polymerization; and secondly, immunodepletion of the complex from extracts completely abolished their responsiveness to GTPγS. Arp2 in extracts is present exclusively as part of the Arp2/3 complex, so we know that anti-Arp2 antibodies affect the function of the entire complex, not just of a pool of free Arp2. Antibodies that do not bind the complex in solution have no effect on polymerization. From experiments with RhoGDI we know that GTPγS stimulates polymerization by activating small GTPases of the Rho family. Anti-Arp2 antibodies also inhibit polymerization activated by Cdc42. We conclude that the Arp2/3 complex is a downstream effector of Cdc42 and of any other Rho-family members that stimulate polymerization in our extracts.

GTPγS-loaded Cdc42, however, does not alter the nucleation activity of purified Arp2/3 complex, indicating that another factor(s) lies between Cdc42 and Arp2/3. Following immunodepletion, addition of purified Arp2/3 complex does not reconstitute GTPγS-stimulated polymerization, suggesting that immunodepletion also removes a cofactor, or possibly that the Arp2/3 complex purified by our methods lacks a required post-translational modification. Mock immunodepletion of the extracts greatly reduced their responsiveness to GTPγS (from more than 40-fold stimulation of actin polymerization to less than 3-fold), probably by removing required phospholipids and membrane-associated proteins. The fact that adding back Arp2/3 complex to immunodepleted extracts does not restore GTPγS responsiveness, therefore, could be a consequence of this general reduction in responsiveness.

Purified Cdc42 was not sufficient to stimulate the nucleation activity of the Arp2/3 complex. Machesky and Insall [49] recently reported that proteins of the Wiskott–Aldrich syndrome protein (WASP) family interact with an Arp2/3 subunit (vertebrate p21-Arc, p18 in *Acanthamoeba* nomenclature) in two-hybrid and affinity chromatography assays. Overexpression of the Arp2/3-binding domain of one WASP family member, Scar1, causes delocalization of the Arp2/3 complex and inhibits lamellipod assembly in cultured mouse fibroblasts. In addition, full-length Scar1 and truncated constructs containing the Arp2/3-binding and actin-binding sites stimulate the nucleation activity of the Arp2/3 complex *in vitro* [50]. Therefore, WASP-family proteins are excellent candidates to form a link between small GTPases and Arp2/3-nucleated actin polymerization.

Our results argue that, in cell extracts, the major mechanism of initiating actin polymerization is *de novo* nucleation mediated by the Arp2/3 complex. The concentration of the Arp2/3 complex in 10-fold dilute extracts is 60 nM. We estimated that the highest concentrations of GTPγS used in our experiments produced approximately 7 nM new barbed ends in these extracts, corresponding to only 10–15% of the total Arp2/3.

Conclusions

From our data we can construct a model of how actin polymerization is regulated in *Acanthamoeba* extracts (Figure 7). In addition to monomeric actin, our model requires factors such as profilin that suppress spontaneous nucleation without inhibiting barbed-end elongation. The model also requires high-affinity capping proteins to inhibit elongation of existing filaments and to terminate G-protein-stimulated polymerization. To initiate polymerization (Figure 7a–c), a nucleation factor must respond to cellular signaling pathways. Exogenous factors, such as the ActA protein from *Listeria monocytogenes*, stimulate the nucleation activity of the Arp2/3 complex [25], but our study provides the first evidence that the Arp2/3 complex is regulated by endogenous cellular signaling pathways. For sustained polymerization, the rate of Arp2/3 activation

Figure 7

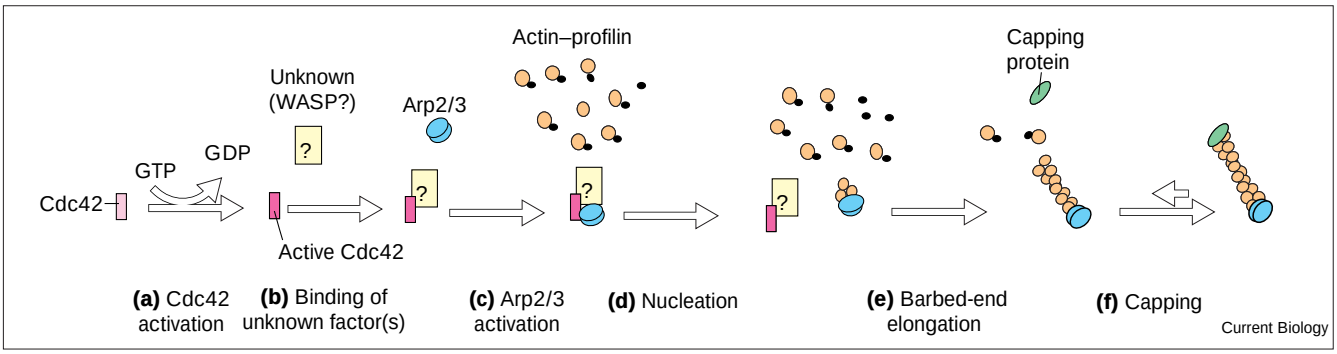

Rho-family GTPase-induced actin polymerization. (a) Cdc42 is activated by exchanging bound GDP for GTP and (b) acts via an unknown intermediate to (c) activate the Arp2/3 complex. Activated Arp2/3 complex then (d) nucleates the formation of new actin filaments. In this model, we show the Arp2/3 complex dissociating from upstream activators because the mechanism of activation appears to be catalytic. Newly formed filaments (e) elongate from their free barbed ends which become (f) capped over time, thereby damping the polymerization response.

and nucleation (Figure 7c,d) must equal or exceed the rate of capping (Figure 7f; equation 5). In *Acanthamoeba* extracts, the Arp2/3 complex appears to be the final downstream effector in G-protein-mediated actin polymerization. A significant challenge remaining in the field of cytoskeletal dynamics is to determine the cellular factors (shown in Figure 7b) that link Rho-family G-protein activation to activation of the Arp2/3 complex.

Materials and methods

Preparation of cell extracts

We grew 1 l cultures of *Acanthamoeba castellanii Neff* to a density of ~2.5×10^6 cells/ml and harvested these log phase cells by centrifugation for 7 min at $3000 \times g$. We washed the cells twice in ice-cold P buffer (50 mM KCl, 340 mM sucrose, 2 mM $MgSO_4$, 1 mM EGTA, 1 mM ATP, 1 mM dithiothreitol (DTT), 10 mM imidazole, pH 7.0) and transferred the packed cells with a clean spatula to an ice-cold Potter–Elvehjem homogenizer (Thomas Scientific). A 1 l culture typically yields 13–15 g of packed cells. Addition of ATP to 1 mM and 0.1 volume of 1 M sucrose made the pellet slightly more fluid, prior to homogenization with 14 strokes of a Teflon plunger at 0 RPM. We centrifuged the extract twice at $150{,}000 \times g$ at 4°C for 1h to remove cell debris and organelles. Filtration of 4–5 ml of extract through a 0.5 ml column of Sepharose 4CL removed large particulate matter. Aliquots of 40–90 µl were quick-frozen in liquid nitrogen and stored at –80°C. Extracts prepared and stored in this manner retained activity for at least a year.

Protein purification and labeling with fluorescent dyes

Acanthamoeba actin was purified from DEAE column fractions by polymerization–depolymerization steps and gel filtration [51]. We purified the Arp2/3 complex from *Acanthamoeba* by ion exchange on DEAE, followed by poly-L-proline affinity chromatography [52]. We purified immunoglobulin G from crude rabbit serum by ammonium-sulfate precipitation followed by DEAE chromatography and then gel filtration on Superdex S200. We labeled actin with pyrene iodoacetamide or rhodamine maleimide (Molecular Probes) [51]. Cdc42 and RhoGDI were gifts from Gary Bokoch and were prepared as previously described [53].

Antibodies and immunoblotting

We previously described the rabbit antibodies with the following specificities: all seven subunits of the *Acanthamoeba* Arp2/3 complex [52]; *Acanthamoeba* Arp2 and Arp3 [54]; and *Acanthamoeba* p35 and p40 [55]. For immunoblot analysis, proteins were subjected to SDS–PAGE [56], electro-transferred [57] to nitrocellulose (BA83; Schleicher & Schuell) and blocked for 1 h in TBS–Tween (0.15 M NaCl, 20 mM Tris–HCl, 0.2% Tween-20) with 3% BSA. We probed the blots with 1:10,000 dilutions of antibodies and secondary horseradish-peroxidase (HRP)-conjugated goat anti-rabbit antibodies (Amersham) in TBS–Tween and detected HRP activity by chemiluminescence. Polyclonal rabbit antibodies against Arp3 (antibody JH47) and Arp2 (antibody JH46) reacted only with their respective antigens on immunoblots of amoeba extracts (Figure 6a), but only the anti-Arp2 antibodies immunoprecipitated the entire Arp2/3 complex. Competition binding experiments using native Arp2/3 complex in solution and denatured Arp2/3 immobilized on multiwell plates revealed the reason for this differential immunoprecipitation. None of the anti-Arp3 antibodies bound the native Arp2/3 complex, but approximately 30% of the anti-Arp2 antibodies recognized native Arp2 within the Arp2/3 complex (Figure 6b). We conclude that some epitopes recognized by anti-Arp2 antibodies are exposed on the surface of the native complex, while all those recognized by anti-Arp3 antibodies are inaccessible. Although they bound the Arp2/3 complex in solution, anti-Arp2 antibodies had no effect on pointed-end capping by Arp2/3 as measured by inhibition of actin elongation from gelsolin-capped seeds by the method of Mullins *et al.* [24].

Measurements of actin polymerization

We measured pyrene–actin fluorescence at an excitation wavelength of 365 nm and emission wavelength of 407 nm using a PTI Alpha-scan spectrafluorometer (Photon Technologies International).

For rhodamine–phalloidin binding, we diluted 10 µl extract into 120 µl P buffer or P buffer containing GTPγS at a final concentration of 200 µM and incubated the mixture for 20 min at 24°C. We added 1 µl buffer containing 0.75 mM rhodamine–phalloidin to each mixture, incubated for 30 min and centrifuged at $350{,}000 \times g$ for 30 min, then washed and resuspended the pellets in 150 mM NaCl, 0.2 mM $MgCl_2$, 10 mM imidazole, pH 7.0. We removed protein by addition of SDS to 1.25%, boiling and centrifugation and quantitated the remaining rhodamine–phalloidin by spectrafluorometry using purified *Acanthamoeba* actin as a standard.

ELISA

We diluted samples into 300 mM NaCl, 10 mM imidazole, pH 7.0 and incubated them in vinyl 96-well microtiter plates (Costar) at 37°C for 1 h. We washed the wells twice with DK buffer (150 mM NaCl, 0.1% Tween 20, and 10 mM Tris–HCl, pH 7.5), blocked with 1% BSA in DK

(DKB buffer) at 37°C for 30 min and washed again four times with DK. We incubated for 1 h at 37°C with anti-Arp2, anti-Arp3, or anti-p40 antibodies at a 1:500 dilution in DKB, washed four more times with DK and incubated for 1 h at 37°C with HRP-conjugated goat anti-rabbit antiserum (Hyclone) diluted 1:2,000 in DKB. Finally, we washed the wells four times with DK and developed with 1 mg/ml *o*-phenylenediamine in phosphate buffer, stopping reactions with 0.5 N H_2SO_4 and reading at 450 nm in a SpectraMax 250 plate reader (Molecular Devices).

Calculation of free barbed ends in extract from pyrene fluorescence data

The rate of polymerization at a given time is described by:

$$\frac{d[F]}{dt} = k_+[E][A] - k_-[E] \quad (6)$$

where [F] is the concentration of polymerized actin, [A] is that of monomeric actin, [E] is that of free barbed ends and k_+ and k_- are the monomer association and dissociation rate constants.

The rate of change in the concentration of free barbed ends with time depends on the rates of nucleation, capping and uncapping:

$$\frac{d[E]}{dt} = -k_{c+}[C][E] + k_{c-}[CE] + \frac{d}{dt}N(t,[GTP\gamma S]) \quad (7)$$

where [CE] is the concentration of capped ends, N is the concentration of nuclei activated by GTPγS, k_{c+} and k_{c-} are the forward and reverse rate constants for capping and [C] is the concentration of capping factors in the extract. The third term, the nucleation rate, is a function of both time and the concentration of GTPγS.

To maintain or induce polymerization, the rates of nucleation and uncapping must simply equal or exceed the rate of capping. Assuming uncapping is slow [12], the rate of formation of nuclei is:

$$\frac{d[N]}{dt} = \frac{d}{dt}\left(\frac{d[F]}{dt}\frac{1}{k_+[A]-k_-}\right) + \frac{k_{c+}[c](k_+[A]-k_-) - k_+\frac{d[A]}{dt}}{(k_+[A]-k_-)^2}\frac{d[F]}{dt} \quad (8)$$

The total number of nuclei at a given time is:

$$N(t) = \frac{d[F]}{dt}\frac{1}{k_+[A]-k_-} + \int_0^t \left[\frac{k_{c+}[c](k_+[A]-k_-) - k_+\frac{d[A]}{d\tau}}{(k_+[A]-k_-)^2}\right]\frac{d[F]}{d\tau}d\tau \quad (9)$$

The first term in equation 9 represents uncapped filaments elongating at a given time. The term under the integral represents nuclei that have formed and been capped up to that time (τ is a dummy variable of integration). We calculated the capping rate in our extracts, $k_{c+}[C]$, from the data in Figure 1 and all other terms in equation 9 are known constants or were calculated from polymerization curves.

Computation

Numerical computations were performed on a Power Macintosh 8500 (Apple) using Microsoft Excel v5.0. Integrals were estimated by the trapezoid rule. Time derivatives of noisy data were estimated by calculating finite differences of data points 10 sec apart, performing a 10-point sliding average of these differences and retaining every 10th value.

Reagents

We bought GTPγS, staurosporine and genistein from Calbiochem, DTT from Boeringer Mannheim, and all salts and buffers, ATP, AMPPNP, leupeptin, pepstatin A, aprotinin and soybean trypsin inhibitor from Sigma. Gary Bokoch of the Scripps Research Institute kindly provided RhoGDI expressed as a GST-fusion protein in *E. coli* and purified using glutathione beads, and Cdc42 expressed in baculovirus-infected SF-9 cells and purified as described [53].

Acknowledgements

This work was supported by NIH research grant GM-26338 to T.D.P. R.D.M. is a fellow of the Jane Coffin Childs Medical Research Foundation. We thank Sally Zigmond and Laura Machesky for helpful conversations and for discussing unpublished data. We are grateful to Gary Bokoch for the generous gifts of Cdc42 and RhoGDI. And we especially thank Laurent Blanchoin for many useful discussions and for pyrene-labeling *Acanthamoeba* actin.

References

1. Tilney LG, Bonder EM, DeRosier DJ: Actin filaments elongate from their membrane-associated ends. *J Cell Biol* 1981, 90:485-494.
2. White JR, Naccache PH, Sha'afi RI: Stimulation by chemoattractant factor of actin associated with the cytoskeleton in rabbit neutrophils. Effects of calcium and cytochalaisin B. *J Biol Chem* 1983, 258:14041-14047.
3. Wang Y: Exchange of actin subunits at the leading edge of living fibroblasts: possible role of treadmilling. *J Cell Biol* 1985, 101:597-602.
4. Mogilner A, Oster G: Cell motility driven by actin polymerization. *Biophys J* 1996, 71:3030-3045.
5. Gerisch G, Fromm H, Huesgen A, Wick U: Control of cell-contact sites by cyclic AMP pulses in differentiating ***Dictyostelium*** cells. *Nature* 1975, 255:547-549.
6. Hartwig JH, Kung S, Kovacsovics T, Janmey PA, Cantley LC, Stossel TP, Toker A: D3 phosphoinositides and outside-in integrin signaling by glycoprotein IIb-IIIa mediate platelet actin assembly and filopodial extension induced by phorbol 12-myristate 13-acetate. *J Biol Chem* 1996, 271:32986-32993.
7. Carlier MF: Control of actin dynamics. *Curr Opin Cell Biol* 1998, 10:45-51.
8. Bray D, Thomas C: Unpolymerized actin in fibroblasts and brain. *J Mol Biol* 1976, 105:527-544.
9. Theriot JA, Mitchison TJ: Actin microfilament dynamics in locomoting cells. *Nature* 1991, 352:126-131.
10. Fechheimer M, Zigmond SH: Focusing on unpolymerized actin. *J Cell Biol* 1993, 123:1-5.
11. Zigmond SH, Joyce M, Yang C, Brown K, Huang M, Pring M: Mechanism of Cdc42-induced actin polymerization in neutrophil extracts. *J Cell Biol* 1998, 142:1001-1012.
12. Schafer DA, Jennings PB, Cooper JA: Dynamics of capping protein and actin assembly in vitro: uncapping barbed ends by polyphosphoinositides. *J Cell Biol* 1996, 135:169-179.
13. Janmey PA, Stossel TP: Modulation of gelsolin function by phosphatidylinositol 4,5-biphosphate. *Nature* 1987, 325:362-364.
14. Eddy RJ, Han J, Condeelis JS: Capping protein terminates but does not initiate chemoattractant-induced actin assembly in ***Dictyostelium***. *J Cell Biol* 1997, 139:1243-1253.
15. Maciver SK, Zot HG, Pollard TD: Characterization of actin filament severing by actophorin from ***Acanthamoeba castellanii***. *J Cell Biol* 1991, 115:1611-1620.
16. Rosenblatt J, Agnew BJ, Abe H, Bamburg JR, Mitchison TJ: ***Xenopus*** actin depolymerizing factor/cofilin (XAC) is responsible for the turnover of actin filaments in ***Listeria monocytogenes*** tails. *J Cell Biol* 1997, 136:1323-1332.
17. Hartwig JH: Mechanisms of actin rearrangements mediating platelet activation. *J Cell Biol* 1992, 118:1421-1442.
18. Hall A: G proteins and small GTPases: distant relatives keep in touch. *Science* 1998, 280:2074-2075.
19. Ridley AJ, Paterson HF, Johnston CL, Diekmann D, Hall A: The small GTP-binding protein rac regulates growth factor-induced membrane ruffling. *Cell* 1992, 70:401-410.
20. Allen WE, Zicha D, Ridley AJ, Jones GE: A role for Cdc42 in macrophage chemotaxis. *J Cell Biol* 1998, 141:1147-1157.
21. Zigmond SH, Joyce M, Borleis J, Bokoch GM, Devreotes PN: Regulation of actin polymerization in cell-free systems by GTPγS and Cdc42. *J Cell Biol* 1997, 138:363-374.
22. Katanaev VL, Wymann MP: GTPgammaS-induced actin polymerisation in vitro: ATP- and phosphoinositide-independent signalling via Rho-family proteins and a plasma membrane-associated guanine nucleotide exchange factor. *J Cell Sci* 1998, 111:1583-1594.

23. Ma L, Cantley LC, Janmey PA, Kirschner MW: Corequirement of specific phosphoinositides and small GTP-binding protein Cdc42 in inducing actin assembly in Xenopus egg extracts. *J Cell Biol* 1998, 140:1125-1136.
24. Mullins RD, Heuser JA, Pollard TD: The interaction of Arp2/3 complex with actin: nucleation, high-affinity pointed end capping, and formation of branching networks of filaments. *Proc Natl Acad Sci USA* 1998, 95:6181-6186.
25. Welch MD, Rosenblatt J, Skoble J, Portnoy DA, Mitchison TJ: Interaction of human Arp2/3 complex and the ***Listeria monocytogenes*** ActA protein in actin filament nucleation. *Science* 1998, 281:105-108.
26. Schwob E, Martin RP: New yeast actin-like gene required late in the cell cycle. *Nature* 1992, 355:179-182.
27. Winter D, Podtelejnikov AV, Mann M, Li R: The complex containing actin-related proteins Arp2 and Arp3 is required for the motility and integrity of yeast actin patches. *Curr Biol* 1997, 7:519-529.
28. Welch MD, Iwamatsu A, Mitchison TJ: Actin polymerization is induced by Arp2/3 protein complex at the surface of ***Listeria monocytogenes***. *Nature* 1997, 385:265-269.
29. Gordon DJ, Eisenberg E, Korn ED: Characterization of a cytoplasmic actin isolated from ***Acanthamoeba castellanii*** by a new method. *J Biol Chem* 1976, 251:4778-4786.
30. Pollard TD: The role of actin in the temperature dependent gelation and contraction of extracts of ***Acanthamoeba***. *J Cell Biol* 1976, 68:579-601.
31. MacLean-Fletcher S, Pollard TD: Viscometric analysis of the gelation of ***Acanthamoeba*** extracts and purification of two gelation factors. *J Cell Biol* 1980, 85:414-428.
32. Holliday LS, Bubb MR, Korn ED: Rabbit skeletal muscle actin behaves differently than A***canthamoeba*** actin when added to soluble extracts of ***Acanthamoeba castellanii***. *Biochem Biophys Res Commun* 1993, 196:569-575.
33. Vinson VK, De La Cruz EM, Higgs HN, Pollard TD: Interactions of Acanthamoeba profilin with actin and nucleotides bound to actin. *Biochemistry* 1998, 37:10871-10880.
34. DiNubile MJ, Cassimeris L, Joyce M, Zigmond SH: Actin filament barbed-end capping activity in neutrophil lysates: the role of capping protein-β2. *Mol Biol Cell* 1995, 6:1659-1671.
35. Isenberg GH, Aebi U, Pollard TD: An actin binding protein from ***Acanthamoeba*** regulates actin filament polymerization and interactions. *Nature* 1980, 288:455-459.
36. Cooper JA, Blum JD, Pollard TD: ***Acanthamoeba castellanii*** capping protein: properties, mechanism of action, immunologic cross-reactivity, and localization. *J Cell Biol* 1984, 99:217-225.
37. Ohga N, Kikuchi A, Ueda T, Yamamoto J, Takai Y: Rabbit intestine contains a protein that inhibits the dissociation of GDP from and the subsequent binding of GTP to rhoB p20, a ras p21-like GTP-binding protein. *Biochem Biophys Res Commun* 1989, 163:1523-1533.
38. Lamarche N, Tapon N, Stowers L, Burbelo PD, Aspenstrom P, Bridges T, *et al.*: Rac and Cdc42 induce actin polymerization and G1 cell cycle progression independently of p65PAK and the JNK/SAPK MAP kinase cascade. *Cell* 1996, 87:519-529.
39. Korn ED: Biochemistry of actomyosin-dependent cell motility. *Proc Natl Acad Sci USA* 1978, 75:588-599.
40. Carlier MF, Laurent V, Santolini J, Melki R, Didry D, Xia GX, *et al.*: Actin depolymerizing factor (ADF/cofilin) enhances the rate of filament turnover: implication in actin-based motility. *J Cell Biol* 1997, 136:1307-1322.
41. Carlsson L, Nyström L-E, Sundkvist I, Markey F, Lindberg U: Actin polymerizability is influenced by profilin, a low molecular weight protein in non-muscle cells. *J Mol Biol* 1977, 115:465-483.
42. Pollard TD, Cooper JA: Quantitative analysis of the effect of ***Acanthamoeba*** profilin on actin filament nucleation and elongation. *Biochemistry* 1984, 23:6631-6641.
43. Tilney LG, Bonder EM, Coluccio LM, Mooseker MS: Actin from ***Thyone briareus*** sperm assembles on only one end of an actin filament: a behavior regulated by profilin. *J Cell Biol* 1983, 97:112-142.
44. Tseng PCH, Runge MS, Cooper JA, Williams RC Jr, Pollard TD: Physical, immunochemical, and functional properties of ***Acanthamoeba*** profilin. *J Cell Biol* 1984, 98:214-221.
45. Goldschmidt-Clermont PJ, Furman MI, Wachsstock D, Safer D, Nachmias VT, Pollard TD: The control of actin nucleotide exchange by thymosinβ4 and profilin. A potential regulatory mechanism for actin polymerization in cells. *Mol Biol Cell* 1992, 3:1015-1024.
46. Safer D, Elzinga M, Nachmias VT: Thymosin beta 4 and Fx, an actin-sequestering peptide, are indistinguishable. *J Biol Chem* 1991, 266:4029-4032.
47. Pantaloni D, Carlier MF: How profilin promotes actin filament assembly in the presence of thymosin β4. *Cell* 1993, 75:1007-1014.
48. Ma L, Rohatgi R, Kirschner MW: The Arp2/3 complex mediates actin polymerization induced by the small GTP-binding protein Cdc42. *Proc Natl Acad Sci USA* 1998, 95:15362-15367.
49. Machesky LM, Insall RH: Scar1 and the related Wiskott-Aldrich Syndrome Protein, WASP, regulate the actin cytoskeleton through Arp2/3 complex. *Curr Biol* 1998, 8:1347-1356.
50. Machesky LM, Mullins RD, Higgs HN, Kaiser DA, Blanchoin L, May RC, *et al.*: WASP-related protein Scar activates dendritic nucleation of actin filaments by Arp2/3 complex. *Proc Natl Acad Sci USA* 1999, 96:3739-3744.
51. Pollard TD: Polymerization of ADP-actin. *J Cell Biol* 1984, 99:769-777.
52. Machesky LM, Atkinson SJ, Ampe C, Vandekerckhove J, Pollard TD: Purification of a cortical complex containing two unconventional actins from ***Acanthamoeba*** by affinity chromatography on profilin agarose. *J Cell Biol* 1994, 127:107-115.
53. Heyworth PG, Knaus UG, Xu DJ, Uhlinger DJ, Conroy L, Bokoch GM, Curnutte JT: Requirement for posttranslational processing of Rac GTP-binding proteins for activation of human neutrophil NADPH oxidase. *Mol Biol Cell* 1993, 4:261-269.
54. Kelleher JF, Atkinson SJ, Pollard TD: Sequences, structural models, and cellular localization of the actin-related proteins Arp2 and Arp3 from Acanthamoeba. *J Cell Biol* 1995, 131:385-397.
55. Mullins RD, Stafford WF, Pollard TD: Structure, subunit topology, and actin-binding activity of the Arp2/3 complex from ***Acanthamoeba***. *J Cell Biol* 1997, 136:331-343.
56. Laemmli UK: Cleavage of structural proteins during the assembly of the head of bacteriophage T4. *Nature* 1970, 227:680-685.
57. Towbin H, Stahelin T, Gordon J: Electrophoretic transfer of proteins from polyacrylamide gels to nitrocellulose sheets: procedures and some applications. *Proc Natl Acad Sci USA* 1979, 76:4350-4354.
58. Folch J, Lees M, Sloane-Stanley GA: *J Biol Chem* 1957, 226:497.
59. Rouser G, Simon G, Kritchevsky G: Species variations in phospholipid class distribution of organs. I. Kidney, liver and spleen. *Lipids* 1969, 4:599-606.
60. Vaskovsky VE, Kostetsky EY: Modified spray for the detection of phospholipids on thin-layer chromatograms. *J Lipid Res* 1968, 9:396.

Because *Current Biology* operates a 'Continuous Publication System' for Research Papers, this paper has been published on the internet before being printed. The paper can be accessed from http://biomednet.com/cbiology/cub – for further information, see the explanation on the contents page.